72nd International Astronautical Congress, Dubai, United Arab Emirates, 25-29 October 2021.

IAC–21–C1.6.4

CISLUNAR ESCAPE TRAJECTORIES THROUGH PATCHED SUN-EARTH/EARTH-MOON THREE-BODY PROBLEM

Andrea Pasquale,[*,a] **Michèle Lavagna,**[b] **Florian Renk**[c]

[a]*Dipartimento di Scienze e Tecnologie Aerospaziali, Politecnico di Milano, Via La Masa, 34, 20156 Milano - Italy*
[b]*Dipartimento di Scienze e Tecnologie Aerospaziali, Politecnico di Milano, Via La Masa, 34, 20156 Milano - Italy*
[c]*ESA/ESOC, Robert-Bosch-Straße 5, 64293 Darmstadt - Germany*

[*] Corresponding Author

Abstract

In the next decade, the exploitation of the Cislunar environment for both manned and unmanned missions will open the space frontier for human exploration of the Moon, Mars and asteroids. The Lunar Gateway (LOP-G) has been proposed as a potential hub for excursions to Mars and activities in support of exploration and planetary defence. Within this context, in this paper, the problem to design a transfer from the Earth-Moon Libration Points to a destination object outside the Cislunar environment is analysed.
In general, the dynamical environment within the Earth-Moon system is rather complex, and the trajectory design is non-trivial. In this study, a further degree of complexity is introduced by the need to patch the escape trajectory with a heliocentric leg, preserving its epoch-dependence. That introduces a phasing problem within the design of the trajectory, which is considered multi-impulsive. Therefore, the problem is split in two steps. First, families of trajectories escaping the Cislunar environment are characterized, to build-up the understanding of the escape mechanisms. Then, a methodology to select the subset of escape trajectories that best match the departure conditions, depending on the epoch and the ΔV available, is applied; relevant applicative cases are discussed in the paper to better highligthen the approach flexibility.

1. Introduction

In the last years, Lunar exploration as been receiving renewed attention as testified by recent NASA's ARTEMIS, and GRAIL missions, and CNSA's Chang'e 3 mission as well as the Lunar Gateway (LOP-G) program. For this reason, in the next years, the Cislunar space is going to become a possible departing outpost for different kinds of exploration missions, including Near-Earth Asteroid Exploration as well as missions to Mars. For this reason, the exploitation of different mechanisms with respect to the *classical* ones has to be exploited, being the trajectories in a multi-body environment.

Many studies have been devoted to the characterisation of Cislunar multi-body orbital families, dedicated to Earth visibility and accessibility [8, 20, 21]. The characterization of escape trajectories from the Cislunar space has also being studied by different authors, exploiting low energy manifolds dynamics [5,11,19], Patched Three-Body Models connecting Earth-Moon Libration Points with Sun-Earth ones [14], Restricted Four Body Models for connecting Earth-Moon Libration Points to Sun-Earth ones or to other regions of the heliocentric space [3, 4, 17] or exploiting solar electric propulsion for NEO exploration missions [9, 18].

This paper presents a novel approach to the generation of initial guesses of Cislunar escape trajectories, exploiting a *patched three-body model* as an higher order alternative of the patched conics model. The approach is aimed to be used to generate sets of initial guesses for the escape trajectories then to be corrected in a full-ephemeris model in a fast and efficient way.

The paper is organized as follows:

- In Section 2, the dynamical models and the reference frames used in the study are presented.
- In Section 3, the Patched Three-Body Model (P3BM) is presented together with the patching conditions and the patching strategy used. The procedure for internal and external trajectory sets generation is also presented.
- In Section 4, a case study for the P3BM is presented and discussed together with the most relevant results.
- In Section 5, the conclusions are presented.

2. Models & Frames

The design of trajectories in the Cislunar space is performed leveraging to different models of increasing complexity: the Circular Restricted Three-Body Problem or CR3BP and the Bi-Circular Restricted Four-Body Problem, or BCR4BP.

2.1 *Reference Frames*

In this work different reference frames are exploited in the trajectory design process. For the sake of clarity, this section reports a brief description of them and the transformations used to pass from one to the other.

ECLIPJ2000 It is the realization of the Mean ecliptic and equinox of J2000. It is the inertial reference frame used in this work. Can be centered at any point of interest (Earth, Sun, Moon, ...).

EM-SYN It is an instantaneous synodic frame associated to the Earth-Moon CR3BP. It is a two-vectors frame built up with the instantaneous Moon position and velocity about the Earth as taken from SPICE `de440` ephemeris. The construction of this frame is largely discussed in literature, therefore is not presented here [13]. With reference to Fig. 2, the EM-SYN frame is the one represented in green.

SE-SYN It is the instantaneous synodic frame associated to the Sun-Earth+Moon CR3BP. In analogy with the EM-SYN frame, it is a two-vectors frame built up with the instantaneous Earth-Moon Barycenter position and velocity about the Sun as taken from SPICE `de440` ephemeris. With reference to Fig. 2, the SE-SYN frame is the one represented in red.

The reference frame transformations are performed directly exploiting SPICE toolkit [1, 2], as the aforementioned reference frame can be found or have been implemented within SPICE environment.

2.2 *Circular Restricted Three-Body Problem*

The Circular Restricted Three-Body Problem (CR3BP) describes the dynamics of a small, massless, third body that moves under the gravitational attraction of two massive bodies, called primaries, in the hypothesis that the primaries moves in a circular orbit about their center of mass. In Fig. 1 is presented the geometry of the problem. The equation of motions are usually expressed in the *synodic reference frame*, which is widely used for trajectory design purposes [16]. Eq 1 shows the equations of motion in the non dimensional form:

$$\begin{cases} \ddot{x} - 2\dot{y} = \mathscr{U}_x \\ \ddot{y} + 2\dot{x} = \mathscr{U}_y \\ \ddot{z} = \mathscr{U}_z \end{cases} \quad [1]$$

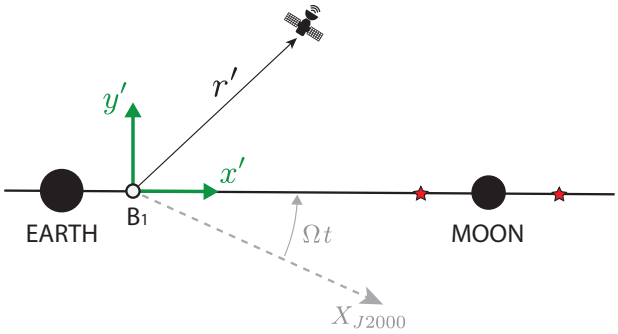

Fig. 1: Circular Restricted Three-Body Problem geometry for the Earth-Moon system.

Here $\dot{(\cdot)}$ and $\ddot{(\cdot)}$ denotes the first and the second derivatives with respect to the (non-dimensional) time, while $\mathscr{U}_{(\cdot)}$ indicates the partial derivative of the pseudopotential function with respect to the variable $(\cdot)$. The pseudopotential is, in this case, defined as:

$$\mathscr{U} = \frac{1}{2}(x^2 + y^2) + \frac{1-\mu}{r_1} + \frac{\mu}{r_2} \quad [2]$$

where r_1 and r_2 represent the distance of the particle from the primaries and μ is the mass ratio.

2.3 *Bi-Circular Restricted Four-Body Problem*

If the motion of the massless particle is assumed to be influenced by the gravitational pull of three bodies instead of two, such as in the context of the trajectory design in the Sun-Earth-Moon system, the Four-Body problem context is exploited. [6] This model assumes that the two primaries P_1 and P_2 revolve in circular orbits about their barycenter (B) and B and the third body P_3 moves in circular orbits around the center of mass of the whole system, B_0. Then, the equations of motion of motion can be written in the Earth-Moon *synodic* frame or in the Sun-Earth one. [11] In the first case, the equations of motion of the CR3BP are modified such that:

$$\begin{cases} \ddot{x}' - 2\dot{y}' = \mathscr{U}_x' - \dfrac{\mu_s}{r_s^3}(x' - x_s) - \dfrac{\mu_s}{a_s^3}x_s \\ \ddot{y}' + 2\dot{x}' = \mathscr{U}_y' - \dfrac{\mu_s}{r_s^3}(y' - y_s) - \dfrac{\mu_s}{a_s^3}y_s \\ \ddot{z}' = \mathscr{U}_z' \end{cases} \quad [3]$$

Note that the Eq. 3 has two additional terms in the planar components which respect to Eq. 1, representing the direct pull of the Sun on the spacecraft and on the Earth-Moon barycenter, respectively. The equation of motion for this case are written in the $\{x', y', z'\}$ synodic frame centered in B_1 (in green in Fig. 3).

$$\begin{cases} \ddot{x}-2\dot{y}=x-\dfrac{1-\mu}{r_s^3}(x+\mu)-\dfrac{\mu(1-\mu')}{r_e^3}(x-(1-\mu)+x_e)-\dfrac{\mu\mu'}{r_m^3}(x-(1-\mu)+x_m) \\ \ddot{y}+2\dot{x}=y-\dfrac{1-\mu}{r_s^3}y-\dfrac{\mu(1-\mu')}{r_e^3}(y+y_e)-\dfrac{\mu\mu'}{r_m^3}(y+y_m) \\ \ddot{z}=-\dfrac{1-\mu}{r_s^3}z-\dfrac{\mu(1-\mu')}{r_e^3}z-\dfrac{\mu\mu'}{r_m^3}z \end{cases} \quad [4]$$

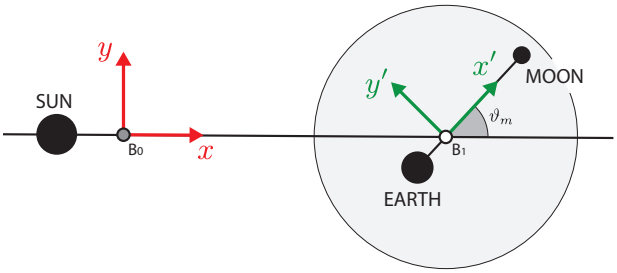

Fig. 2: Bi-Circular Restricted Four-Body Problem geometry for the Sun-Earth-Moon system.

Another formulation of the BCR4BP, instead, considers the Moon as a perturbation of the Sun-Earth CR3BP. In this case, the equation of motion can be written in the Sun-Earth synodic frame $\{x,y,z\}$ centered in B_0 (in red in Fig. 2), and are presented in Eq. 4. In this case, with μ is denoted the mass ratio of the Sun-Earth(+Moon) CR3BP and with μ' the mass one of the Earth-Moon CR3BP.

With reference to Fig. 2, the cartesian position of the Earth and the Moon which respect to the Earth-Moon barycenter (B_1) can be recovered by:

$$\begin{aligned} x_e &= -\mu' l^* \cos\vartheta_m \\ y_e &= -\mu' l^* \sin\vartheta_m \\ x_m &= (1-\mu') l^* \cos\vartheta_m \\ y_m &= (1-\mu') l^* \sin\vartheta_m \end{aligned} \quad [5]$$

Where ϑ_m is the Moon angular position which respect to the Sun-B_1 x synodic axis, taken positive counterclockwise and l^* is the non-dimensional Earth-Moon distance.

Note that in both formulations, the equations of motion are not-coherent. That is, the assumed motions do not satisfy Newton's equations. However, this model is extremely useful for the design of trajectories within the Sun-Earth-Moon system and provide accurate insight of a full-ephemeris environment, thus is compared to the proposed Patched-CR3BP approach.

3. The Patched Three-Body Model

In this study a *higher-order* alternative of the patched conics model, called Patched (Bi)-Circular Restricted Three Body Model or P3BM, is proposed and exploited for the design of escape trajectories from the Cislunar space. This approach is preferred over a direct design of the escape trajectories within the BCR4BP for two main reasons:

1. The possibility to decouple the design of the escape, from the interplanetary trajectory. This allow to split the problem in two distinct legs:

   - the **Internal Problem** (IP): starting from the departure point up to a given switching radius, is the Cislunar leg of the trajectory; it can be a direct escape from Libration Point Orbit (LPO) or include one or multiple flybys of the Earth or the Moon.
   - the **External Problem** (EP): is associated to the heliocentric leg of the trajectory, from the selected switching radius up to the target interception.

2. The possibility to preliminary design the trajectories within two autonomous dynamical systems, instead of a non-autonomous one. This is extremely beneficial, since there is a large number of Dynamical System Theory tools which works really well with autonomous systems.

3.1 *Switching Surface*

The P3BM can be specified once a **switching surface**, $\mathscr{S}$, between the IP and the EP is assigned. In literature a similar concept has been called *Sphere of Equivalence* (SOE) by other authors [7]. However, the switching surface exploited in this work is an *abstract* concept, not a physical one, as explained afterwards.

First, the SOE concept is introduced: it represents a mathematical surface where the IP-model gravity vector field is *equivalent* to a two-body vector field. The surface is here build in the EM-SYN frame, considering the IP

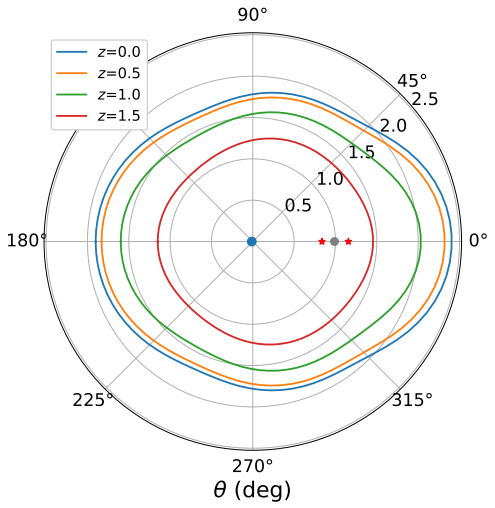

Fig. 3: SOE in the synodic frame (polar axis).

gravitational acceleration:

$$\mathbf{a}_{IP} = \begin{pmatrix} x - \dfrac{1-\mu}{r_e^3}(x+x_e) - \dfrac{\mu}{r_m^3}(x+x_m) \\ y - \dfrac{1-\mu}{r_e^3}y - \dfrac{\mu}{r_m^3}y \\ -\dfrac{1-\mu}{r_e^3}z - \dfrac{\mu}{r_m^3}z \end{pmatrix} \quad [6]$$

and its equivalent Two-Body representation:

$$\mathbf{a}_{2B} = \begin{pmatrix} x \\ y \\ 0 \end{pmatrix} - \frac{1}{r^3}\begin{pmatrix} x \\ y \\ z \end{pmatrix} \quad [7]$$

Note that here all quantities are in Earth-Moon CR3BP non-dimensional units. With those definitions, the SOE can be defined as:

$$\mathscr{S}(x,y,z) = \frac{||\mathbf{a}_{IP} - \mathbf{a}_{2B}||}{||\mathbf{a}_{IP}||} \quad [8]$$

A representation of the SOE is presented in Fig. 3, as a function of the out-of-plane component, z. As expected, the SOE is more prominent along the positive x axis, where it reaches 2.5 non-dimensional units. This is due to the presence of the Moon at $x = 1-\mu$

However, if the SOE would be adopted as switching surface, the patching would be asymmetric, meaning that there would be a direct dependence of the legs on θ_m. This is something not desired, since such a coupling would act against the exploitation of the P3BM. In fact, in case the SOE is used as switching surface, both the IP and the EP would have a dependency on ϑ_m. For those reasons, a **spherical surface** is considered as switching surface. Introducing this simplification allow to remove the direct dependency on ϑ_m, enabling the possibility to generate EP/IP arcs independently. A switching surface $\mathscr{S}$, centred in B_1 with radius $R_c = 2R_{\text{SOI}}$ is then considered.

On the switching surface, vector quantities that has to be matched can be generally denoted with $\mathbf{q}^+$ if belonging to the EP, and $\mathbf{q}^-$ if associated to the IP.

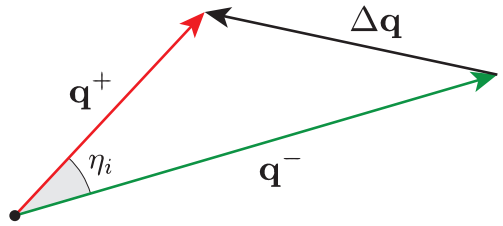

Fig. 4: Internal/external vector patching triangles.

Then, the η_q angle, between the IP and the EP vectors can be defined as:

$$\eta_q = \arccos \frac{\mathbf{q}^+ \cdot \mathbf{q}^-}{||\mathbf{q}^+||\,||\mathbf{q}^-||} \quad [9]$$

and the vector difference:

$$\Delta\mathbf{q} = \mathbf{q}^+ - \mathbf{q}^- \quad [10]$$

defines the vector defect between the internal and the external quantities.

3.2 *Patching Conditions*

Different quantities are exploited to assess the quality of the patching. In general a patching quantity referred to an internal γ_j trajectory and an external γ_i trajectory is called q_{ij}. A *perfect* patching is achieved between the two trajectories if *all* $q_{ij} = 0$.

The following quantities are used in this study:

1. δ_v: it is directly associated to the magnitude of the hyperbolic excess velocity magnitude of the IP and the EP trajectories. It is defined as:

$$\delta_v = 1 - \frac{V_\infty^+}{V_\infty^-} \quad [11]$$

where here $V_\infty^{(\cdot)}$ is the modulus of the barycentric inertial velocity computed at the switching sphere.

2. δ_r: it is the normalized difference in the position vectors in the SE-SYN frame of a tuple of IP/sEP trajectories. It is defined as:

$$\delta_r = \frac{\Delta\mathbf{r}}{l^*} = \frac{||\mathbf{r}^+ - \mathbf{r}^-(\vartheta_m)||}{l^*} \quad [12]$$

3. $\bar{\eta}_r$: it is the normalized angle between the IP/EP position vectors in the SE-SYN frame, defined as:

$$\bar{\eta}_r = \frac{1}{\pi}\eta_r = \frac{1}{\pi}\arccos\frac{\mathbf{r}^+\cdot\mathbf{r}^-(\vartheta_m)}{r^+ r^-(\vartheta_m)} \qquad [13]$$

The position vectors are here expressed with respect to B_1.

4. $\bar{\eta}_v$: it is the normalized angle between the IP/EP velocity vectors in the SE-SYN frame, defined as:

$$\bar{\eta}_v = \frac{1}{\pi}\eta_v = \frac{1}{\pi}\arccos\frac{\mathbf{v}^+\cdot\mathbf{v}^-(\vartheta_m)}{v^+ v^-(\vartheta_m)} \qquad [14]$$

Since the objective of the P-CR3BM is to provide reasonably good initial guesses of patched trajectories, it is assumed a trajectory to be perfectly patched if *all* $q_{ij} \leq \varepsilon$. In this work it is assumed that:

- for δ_r, which is expressed in SE-CR3BP non dimensional quantities ε_r is imposed to $1e-4$, which corresponds approximately to 15 000 km.
- for $|\delta_v|$, ε_δ is imposed to 0.05, thus considering a 5% error in V_∞.
- for $|\bar{\eta}_r|$, ε_η is imposed to 0.01, allowing for a position misalignment of $\pm 1.8°$.
- finally, since the proposed patching method is intended as a tool to generate initial guesses to be corrected within a Differential Correction algorithm, the velocity misalignment tolerance ε_η is relaxed to 0.25, allowing for a misalignment of $\pm 45°$.

3.3 *Patching Strategy*

In this section, the general strategy proposed for the generation of the patched trajectories is discussed. This approach relays on the generation of two databases:

- The **External Trajectory Set**, $(\gamma_0,\dots,\gamma_i,\dots,\gamma_n)$, composed by the EP trajectories, generated by means of a pork-chop plots.
- The **Internal Trajectory Set**, $(\gamma_0,\dots,\gamma_i,\dots,\gamma_m)$, composed by different families of escape trajectories, which design is briefly described afterwards.

Once the two databases are available, the patching conditions are used to filter it an recover the subset of trajectories considered to be correctly patched. Note that the proposed patching conditions depends on both IP/EP trajectories as well as on the Moon angle, ϑ_m. However, when a tuple (γ_i,γ_j) is assigned, all the patching quantities can be evaluated: once the Epoch of γ_i at the switching surface is assigned, then the Moon angle for all the associated γ_j can be recovered.

After that, a set of patched trajectories $(\dots,(\gamma_i,\gamma_j),\dots)$ is obtained and passed to a Multiple Shooting Method, to recover the final set of corrected trajectories.

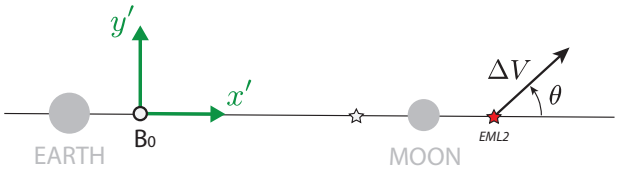

Fig. 5: EML2 escape maneuver geometry.

3.4 *External Trajectory Set*

This set is simply generated assuming Two-Body motion of the Earth and the target body around the Sun and exploiting Lambert problem [15]. In particular, having assigned a departure window of interest and a Time of Flight (TOF) span, a pork-chop plot for the transfer can be easily built. Then, on the basis of a parameter of merit p (that can be V_∞, total ΔV or something else), the trajectories belonging to the pork-chop can be filtered, resulting in the subset:

$$\mathscr{G}_{\text{ext}} = (\tilde{\gamma}_0,\dots,\tilde{\gamma}_i,\dots,\tilde{\gamma}_n) \qquad [15]$$

Each member of this set is characterized by means of the final state vector at the target interception ($\mathbf{X}_t$), in the ECLIPJ2000 frame and the arrival Epoch, E_t. In order to pass from the patched conics to the proposed P3BM a further step is performed: for each member of the set $\mathscr{G}_{\text{ext}}$, $\mathbf{X}_t$ is firstly converted into the SE-SYN frame, $\tilde{\mathbf{x}}_t^+$, and then propagated backward in time up to the switching surface, to obtain the state at the interception, $\mathbf{x}_0^+$.

In general, it is not guaranteed that the backward-propagation of $\tilde{\mathbf{x}}_t^+$ would effectively result in a switching surface interception. For this reason a correction layer is added: a simple Differential Evolution optimisation step is considered [10], given as design variables a vector $\delta \in \mathbb{R}^3$, such that the corrected target interception state is given by:

$$\mathbf{x}_t^+ = \tilde{\mathbf{x}}_t^+ + \mathbb{D}\,\delta \qquad [16]$$

3.5 *Internal Trajectory Set*

For the generation of Cislunar escape trajectories, different mechanisms can be exploited. Among the others:

- Direct escapes through a maneuver on the Libration Points. [12]

- Indirect Escape through a Earth/Moon powered flyby.
- Other low-energy mechanisms. [17]

In this work, the effectiveness of the method is tested through the exploitation of direct escapes, since the method more than the escape mechanisms is analysed. Then, the generation of direct escape trajectories from the EML2 Libration Point is performed as a function of $(\Delta V, \theta)$, where ΔV is the maneuvering magnitude and θ is the in-plane maneuvering angle from the x EM-SYN axis, as shown in Fig. 5. In particular, the escape set is generated as follows:

1. Assuming to start at one of Earth-Moon Lagrangian Points, a manoeuvre is performed, with a given magnitude ΔV and directed with a given angle θ, computed positively from the x-axis of the Earth-Moon rotating frame.
2. The trajectory is propagated until it reaches the switching surface. A maximum time of 3 months is considered, to capture also *low-energy*, multi-revolution escape dynamics.
3. The state at the control surface is gathered, to be used as a figure of merit.

A full scan of 360 deg span for the θ angle and a $0\,\mathrm{km/s}$ to $2.5\,\mathrm{km/s}$ span for the Δv is performed, with the following parameters considered as figures of merit:

- Osculating eccentricity, e_{EMB} at a control point on the switching surface.
- Time of fight to reach the control surface, t_{ESC}, representing the time needed to escape from the region where the Earth-Moon gravity is dominant.
- The ratio $V_\infty/\Delta v$, called *escape velocity efficiency*, where V_∞ is the barycentric velocity at the control point, representing the equivalent outgoing asymptote.
- The minimum altitude to the Moon h_{MOON} with $t \in [0, t_{\mathrm{ESC}}]$.
- The minimum altitude to the Earth h_{EARTH} with $t \in [0, t_{\mathrm{ESC}}]$.

In Fig. 6, the most relevant figures of merit for a direct EML2 escape are presented. Note that, thanks to the nature of the problem, some efficient trajectories could be obtained ($V_\infty/\Delta V > 1$), if the maneuver is performed in the correct direction with an appropriate magnitude.

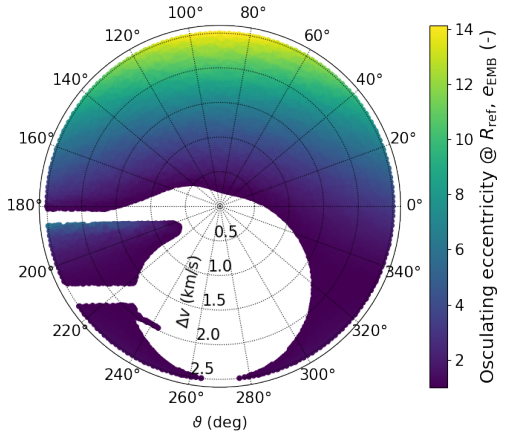

(a)

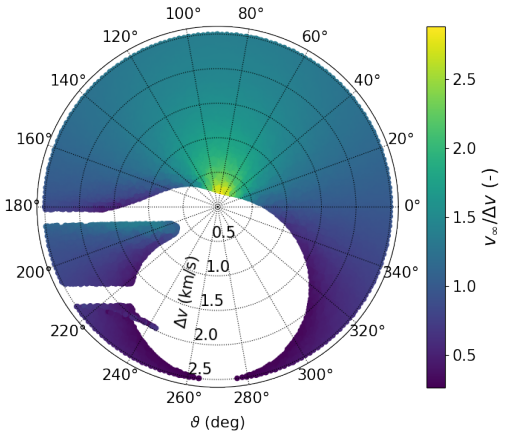

(b)

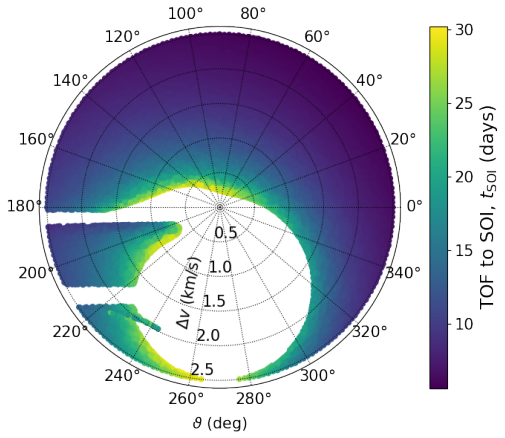

(c)

Fig. 6: EML2 Direct escape figure of merits.

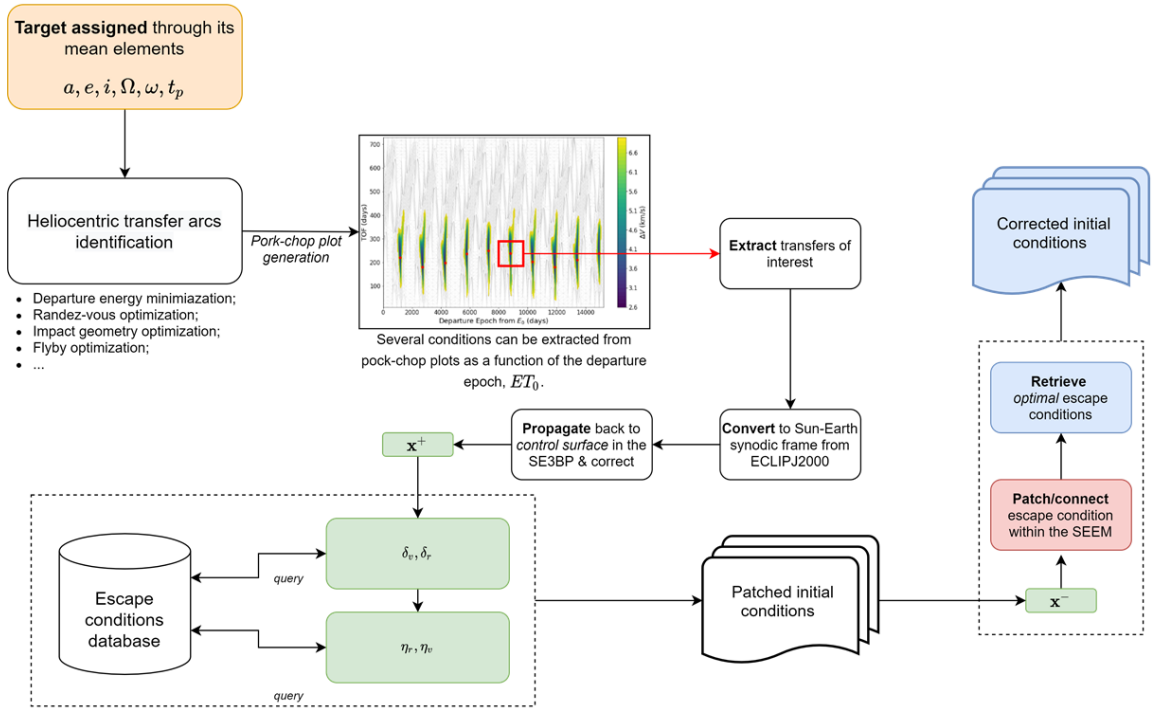

Fig. 7: P3BM procedure

4. Case Study

As a case study, a fly-by mission to a Near-Earth Asteroid (NEA) with semimajor axis of 1.05 AU, an eccentricity of 0.5 and an inclination of 5 deg is considered. Therefore, the P3BM is considered for the design of a EML2 direct escape toward the target. Following the procedure presented in Fig. 7, the following steps are performed:

1. The pork-chop plot for the transfer towards the target is generated, assuming the reference Epoch ET_0 as *2022-01-01 00:00:00*. Fig. 8 shows the pork-chop plot as well as the moon angle ϑ_m as a function of the Epoch. Note that the regions where the minima are located are approximately at a moon angle of 180 deg.

2. Backward propagate and correct the external problem trajectories within the Sun-Earth-Moon BCR4BP, to obtain the external trajectory set. From this step, a group of states and Epochs couples at the switching surface are obtained.

3. The internal trajectory set databases are loaded. In this case only direct escapes from EML2 are considered, but the procedure can be easily extended to any kind of internal problem trajectories.

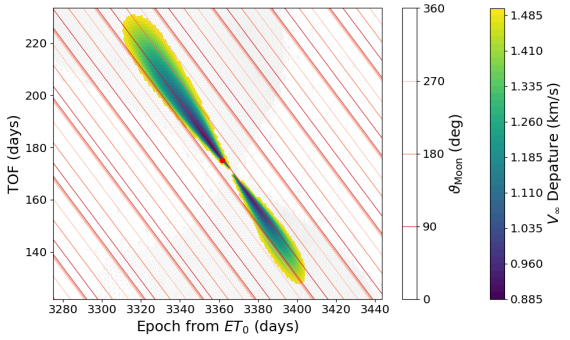

Fig. 8: NEA fly-by mission pork-chop plot.

4. The patching conditions are applied to each trajectories couple (γ_i, γ_j), where γ_i belongs to the internal trajectory set and γ_j to the external one. In Fig. 9 the results of the applications of the patching conditions is presented:

   - First, the patched-conics-like alternatives (i.e. imposing only δ_v) are retrieved and plotted in blue for a subset of the escape database ($\Delta V < 1.25\,\mathrm{km/s}$).
   - Then, all the patching conditions are applied.

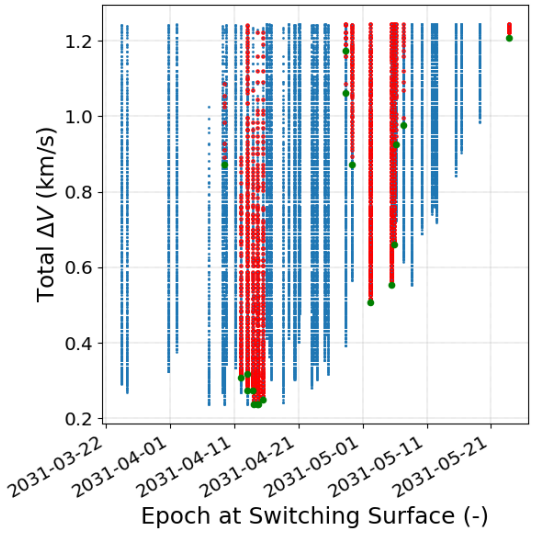

Fig. 9: P3BM solutions front.

This restricts the domain of the solutions to the red points presented on the figure. Note that the dependency of the solutions on the Epoch increases here.

- Finally, the P3BM alternatives with the minimum ΔV are extracted. These points are represented in green on the same figure.

5. The P3BM solutions are corrected in a multiple shooting or optimized with a collocation method for NLP. As an example, in Fig. 10 are presented the corrected solution obtained starting from the patched trajectories and Fig. 11 shows the corrected trajectories.

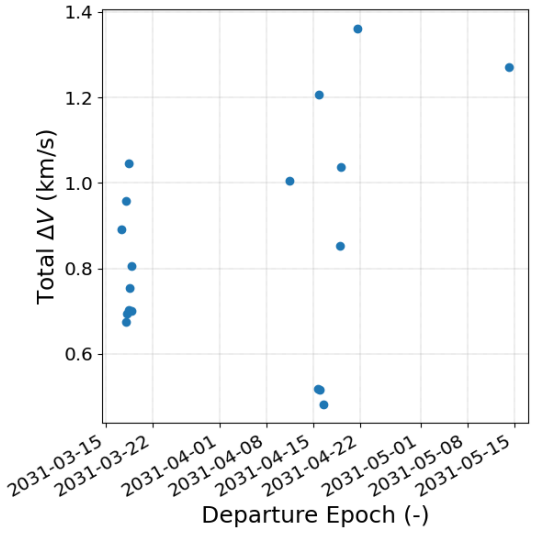

Fig. 10: P3BM corrected solutions.

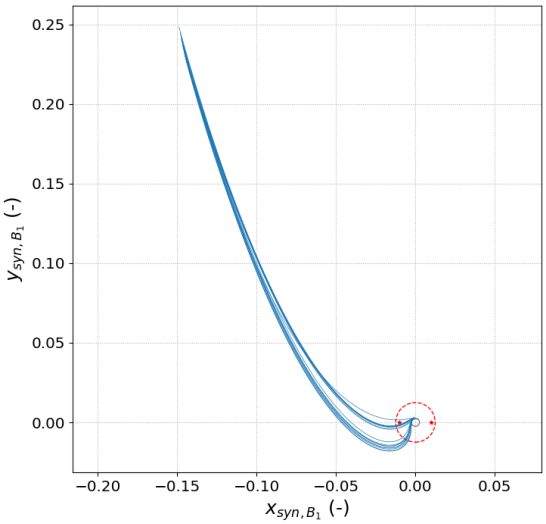

Fig. 11: P3BM corrected trajectories in the SE-SYN frame, centered at the Earth-Moon barycenter.

5. Conclusions

In this paper, the definition of a new Patched Three-Body Model together with a relevant application have been presented. First, the definition of patching conditions based on the actual patching geometry are presented and discussed. Then, the mechanisms for the generation of the initial condition through the P3BM is described and applied to a NEA fly-by mission example.

The method appears to be really flexible, since the escape conditions can be build once and then used for different mission scenarios. Moreover, the application of the patching conditions guarantee a fast convergence of the correction procedure, allowing for a fast identification of suitable escape trajectories from the Cislunar space toward any kind of object in the heliocentric space.

6. Acknowledgements

The research is carried out with the European Space Operations Centre, under the Networking/Partnering Initiative (NPI) between Politecnico di Milano and the European Space Agency.

References

[1] Charles H Acton Jr. Ancillary data services of nasa's navigation and ancillary information facility. *Planetary and Space Science*, 44(1):65–70, 1996.

[2] Andrew M Annex, Ben Pearson, Benoît Seignovert, Brian T Carcich, Helge Eichhorn, Jesse A Mapel, Johan L Freiherr Von Forstner, Jonathan McAuliffe, Jorge Diaz Del Rio, Kristin L Berry, et al. Spiceypy: a pythonic wrapper for the spice toolkit. *Journal of Open Source Software*, 5(46):2050, 2020.

[3] Kenza Boudad, Kathleen Howell, and Diane Davis. Energy and phasing considerations for low-energy transfers from cislunar to heliocentric space.

[4] Kenza Boudad, Kathleen Howell, and Diane Davis. Heliocentric access from cislunar space within the context of the bicircular restricted four-body problem. In *AAS/AIAA Astrodynamics Specialist Conference, Lake Tahoe, California (Virtual)*, 2020.

[5] Davide Conte, Marilena Di Carlo, Koki Ho, David B Spencer, and Massimiliano Vasile. Earth-mars transfers through moon distant retrograde orbits. *Acta Astronautica*, 143:372–379, 2018.

[6] Diogene Alessandro Dei Tos and Francesco Topputo. On the advantages of exploiting the hierarchical structure of astrodynamical models. *Acta Astronautica*, 136:236–247, 2017.

[7] Fabio Ferrari, Michèle Lavagna, and Kathleen C Howell. Dynamical model of binary asteroid systems through patched three-body problems. *Celestial Mechanics and Dynamical Astronomy*, 125(4):413–433, 2016.

[8] D.J. Grebow. Generating periodic orbits in the circular restricted three-body problem with applications to lunar south pole coverage, 2006.

[9] C. Greco, M. Di Carlo, L. Walker, and M. Vasile. Analysis of neos reachability with nano-satellites and low-thrust propulsion. In *Small Satellites, Systems and Services Symposium*, Sorrento, Italy, 2018, 2018.

[10] Derviş Karaboğa and Selçuk Ökdem. A simple and global optimization algorithm for engineering problems: differential evolution algorithm. *Turkish Journal of Electrical Engineering & Computer Sciences*, 12(1):53–60, 2004.

[11] Wang Sang Koon, Martin W Lo, Jerrold E Marsden, and Shane D Ross. Dynamical systems, the three-body problem and space mission design. In *Equadiff 99: (In 2 Volumes)*, pages 1167–1181. World Scientific, 2000.

[12] Andrea Pasquale, Florian Renk, and Michèle Lavagna. Cislunar departure exploitation for planetary defense missions design. In *Planetary Defense Conference*, 05 2021.

[13] Thomas A Pavlak. *Mission design applications in the earth-moon system: Transfer trajectories and stationkeeping*. Purdue University, 2010.

[14] Hao Peng, Xiaoli Bai, Josep J Masdemont, Gerard Gómez, and Shijie Xu. Libration transfer design using patched elliptic three-body models and graphics processing units. *Journal of Guidance, Control, and Dynamics*, 40(12):3155–3166, 2017.

[15] Ryan P Russell. On the solution to every lambert problem. *Celestial Mechanics and Dynamical Astronomy*, 131(11):1–33, 2019.

[16] V. Szebehely. *Theory of Orbits: The Restricted Problem of Three Bodies*. Academic Press, New York and London, 1967.

[17] Keita Tanaka and Jun'Ichiro Kawaguchi. Escape trajectories from the l2 point of the earth-moon system. *Transactions of the Japan Society for Aeronautical and Space Sciences*, 57(4):238–244, 2014.

[18] Francesco Topputo, Yang Wang, Carmine Giordano, Vittorio Franzese, Hannah Goldberg, Franco Perez-Lissi, and Roger Walker. Envelop of reachable asteroids by m-argo cubesat. *Advances in Space Research*, 2021.

[19] Shuai Wang, HaiBin Shang, and WeiRen Wu. Interplanetary transfers employing invariant manifolds and gravity assist between periodic orbits. *Science China Technological Sciences*, 56(3):786–794, 2013.

[20] Jacob Williams, David E Lee, Ryan J Whitley, Kevin A Bokelmann, Diane C Davis, and Christopher F Berry. Targeting cislunar near rectilinear halo orbits for human space exploration. 2017.

[21] Emily M Zimovan, Kathleen C Howell, and Diane C Davis. Near rectilinear halo orbits and their application in cis-lunar space. In *3rd IAA Conference on Dynamics and Control of Space Systems, Moscow, Russia*, volume 20, 2017.